

# Beta-Carotene Reduces Body Adiposity of Mice via BCMO1

Jaume Amengual<sup>1,2,3</sup>, Erwan Gouranton<sup>3,9</sup>, Yvonne G. J. van Helden<sup>4,5,6,9</sup>, Susanne Hessel<sup>7</sup>, Joan Ribot<sup>1</sup>, Evelien Kramer<sup>6</sup>, Beata Kiec-Wilk<sup>8</sup>, Ursula Razny<sup>8</sup>, Georg Lietz<sup>9</sup>, Adrian Wyss<sup>10</sup>, Aldona Dembinska-Kiec<sup>8</sup>, Andreu Palou<sup>1</sup>, Jaap Keijer<sup>3</sup>, Jean François Landrier<sup>3</sup>, M. Luisa Bonet<sup>1\*</sup>, Johannes von Lintig<sup>7,2\*</sup>

**1** Laboratory of Molecular Biology, Nutrition and Biotechnology, Universitat de les Illes Balears and CIBER de Fisiopatología de la Obesidad y Nutrición (CIBERObn), Palma de Mallorca, Spain, **2** Department of Pharmacology, School of Medicine, Case Western Reserve University, Cleveland, Ohio United States of America, **3** INRA, UMR 1260 Nutriments Lipidiques et Prevention des Maladies Métaboliques/Université Aix-Marseille 1 et II, Marseille, France, **4** Human and Animal Physiology, Wageningen University, Wageningen, The Netherlands, **5** University Maastricht, Maastricht, The Netherlands, **6** RIKILT-Institute of Food Safety, Wageningen, The Netherlands, **7** Institute of Biology I, University of Freiburg, Freiburg, Germany, **8** Department of Clinical Biochemistry, The Jagiellonian University Medical College, Krakow, Poland, **9** School of AFRD, Newcastle University, Newcastle upon Tyne, United Kingdom, **10** DSM Nutritional Products, R&D Human Nutrition and Health, Kaiseraugst, Switzerland

## Abstract

Evidence from cell culture studies indicates that  $\beta$ -carotene (BC)-derived apocarotenoid signaling molecules can modulate the activities of nuclear receptors that regulate many aspects of adipocyte physiology. Two BC metabolizing enzymes, the BC-15,15'-oxygenase (*Bcmo1*) and the BC-9',10'-oxygenase (*Bcdo2*) are expressed in adipocytes. *Bcmo1* catalyzes the conversion of BC into retinaldehyde and *Bcdo2* into  $\beta$ -10'-apocarotenol and  $\beta$ -ionone. Here we analyzed the impact of BC on body adiposity of mice. To genetically dissect the roles of *Bcmo1* and *Bcdo2* in this process, we used wild-type and *Bcmo1*<sup>-/-</sup> mice for this study. In wild-type mice, BC was converted into retinoids. In contrast, *Bcmo1*<sup>-/-</sup> mice showed increased expression of *Bcdo2* in adipocytes and  $\beta$ -10'-apocarotenol accumulated as the major BC derivative. In wild-type mice, BC significantly reduced body adiposity (by 28%), leptinemia and adipocyte size. Genome wide microarray analysis of inguinal white adipose tissue revealed a generalized decrease of mRNA expression of peroxisome proliferator-activated receptor  $\gamma$  (PPAR $\gamma$ ) target genes. Consistently, the expression of this key transcription factor for lipogenesis was significantly reduced both on the mRNA and protein levels. Despite  $\beta$ -10'-apocarotenoid production, this effect of BC was absent in *Bcmo1*<sup>-/-</sup> mice, demonstrating that it was dependent on the *Bcmo1*-mediated production of retinoids. Our study evidences an important role of BC for the control of body adiposity in mice and identifies *Bcmo1* as critical molecular player for the regulation of PPAR $\gamma$  activity in adipocytes

**Citation:** Amengual J, Gouranton E, van Helden YGJ, Hessel S, Ribot J, et al. (2011) Beta-Carotene Reduces Body Adiposity of Mice via BCMO1. PLoS ONE 6(6): e20644. doi:10.1371/journal.pone.0020644

**Editor:** Rakesh K. Srivastava, The University of Kansas Medical center, United States of America

**Received:** February 9, 2011; **Accepted:** May 5, 2011; **Published:** June 1, 2011

**Copyright:** © 2011 Amengual et al. This is an open-access article distributed under the terms of the Creative Commons Attribution License, which permits unrestricted use, distribution, and reproduction in any medium, provided the original author and source are credited.

**Funding:** This work was developed as part of The European Nutrigenomics Organisation (Network of Excellence, EU Contract FOOD-CT-2004-506360) Focus Team 9 "Window of Benefit for Carotenoids" coordinated by Georg Lietz, and has been sponsored in part by NuGO. It has also been supported by the Spanish Government (Ministerio de Educación y Ciencia, grant AGL2006-04887/ALI and AGL2009-11277/ALI to Andreu Palou) and by INRA and INSERM (France). CIBERObn is an initiative of the Instituto de Salud Carlos III (Spanish Government). Jaap Keijer, Andreu Palou and Aldona Dembinska-Kiec are members of Mitofood (Cost Action F0602). Jaume Amengual was a fellow from the Spanish Government. Yvonne van Helden is supported by VLAG/Nutrim. The funders had no role in study design, data collection and analysis, decision to publish, or preparation of the manuscript.

**Competing Interests:** The authors have declared that no competing interests exist.

\* E-mail: luisabonet@uib.es (MLB); johannes.vonlintig@case.edu (JVL)

† These authors contributed equally to this work.

## Introduction

In mammals,  $\beta$ -carotene (BC) is the natural precursor for apocarotenoids molecules including retinoids (vitamin A and its derivatives) [1]. Two different types of BC metabolizing enzymes have been identified that are expressed in various tissues [2-4]. The  $\beta$ -carotene-15,15'-monooxygenase (*Bcmo1*) converts BC to all-*trans*-retinal [5;6] and studies in knockout (*Bcmo1*<sup>-/-</sup>) mice show that *Bcmo1* is the primary enzyme for retinoid production [7-9]. Besides *Bcmo1*, mammalian genomes encode a second BC metabolizing enzyme known as  $\beta$ -carotene-9',10'-dioxygenase (*Bcdo2*). *Bcdo2* cleaves BC at position 9,10, resulting in the formation of one molecule  $\beta$ -ionone and one molecule  $\beta$ -10'-apocarotenol [4].

Increasing evidence has been provided that BC-derived apocarotenoid signaling molecule can influence adipocyte

physiology. *Bcmo1* knockout mice are highly susceptible to high fat diet-induced obesity and show increased expression of peroxisome proliferator-activated receptor  $\gamma$  (PPAR $\gamma$ ) regulated genes in fat depots [7]. PPARs control the expression of genes for lipid and glucose metabolism [10;11] and PPAR $\gamma$  is pivotal for adipocyte differentiation and lipogenesis in mature adipocytes [12]. *Bcmo1* gene expression is under the control of PPAR $\gamma$  [13;14] and is induced during adipocyte differentiation [15]. The primary BC cleavage product retinaldehyde has been shown to inhibit PPAR $\gamma$  activity both in adipocyte cell cultures and mouse models [16]. Furthermore, evidence has been provided that *Bcmo1* plays an important role for retinoic acid production and retinoic acid receptor (RAR) signaling in adipocytes [15]. Retinoic acid influences adipocyte differentiation [17;18] and fat deposition [19], mitochondrial uncoupling [20;21], oxidative metabolism [22;23] and the expression of

adipokines such as leptin, resistin, and serum retinol binding protein [24–27]. Part of these effects are mediated via RARs, which upon retinoic acid binding regulate the expression of direct target genes [28] and interfere with the activity of other transcription factors, including early adipogenic transcription factors such as PPAR $\gamma$  [17;18]. In addition, retinoic acid may influence PPAR-mediated responses by activating the retinoid X receptor (RXR) moiety of permissive PPAR:RXR heterodimers [29] and, possibly, by serving as an agonist of PPAR $\beta/\delta$  [30;31]. Finally, BC-derived long chain apocarotenoids such as  $\beta$ -apo-14'-carotenal can inhibit PPAR $\gamma$  activity and adipogenesis in cell culture [32]. Moreover,  $\beta$ -13-apocarotenone has been shown to inhibit RXR $\alpha$  activity [33].

These findings implicate that a tissue-specific conversion of BC via carotenoid-oxygenases can influence the activities of key transcription factor that control adipocyte physiology. However, this concept lacks experimental testing in animal models. Here we wished to systematically analyze the effects of BC on the adipose phenotype in mice. To genetically dissect the contributions of *Bcmo1* and *Bcdo2* to this process, we used wild-type (WT) and *Bcmo1*<sup>-/-</sup> mice in this study. Our analysis included a genome wide expression analysis of inguinal white adipose tissue (iWAT) to identify the target genes of BC action in this tissue.

## Results

### Effects of dietary BC supplementation on BC and retinoid levels in serum and adipose tissue

Five-week-old WT and *Bcmo1*<sup>-/-</sup> female mice were fed a defined, pelleted diet containing 1500 IU vitamin A/kg with (BC diet) or without (control diet) 150 mg BC/kg diet (n=6 animals per group). After 14 weeks, we first studied expression of *Bcmo1* in iWAT of different dietary groups and genotypes. *Bcmo1* was expressed in iWAT of WT but not *Bcmo1*<sup>-/-</sup> mice (Figure 1A). We also analyzed the mRNA expression levels of *Bcdo2*, which encodes a second carotenoid metabolizing enzyme [5]. This analysis revealed a marked up-regulation of *Bcdo2* expression in iWAT of *Bcmo1*-null mice, both with control and BC diet (Figure 1B). Similar results were obtained for *Bcmo1* and *Bcdo2* expression in gonadal WAT (Figure S1).

Serum and iWAT BC levels were significantly increased after the 14 weeks of dietary intervention in all animals subjected to BC supplementation (Figures 1C and 1E). This increase was much more pronounced in the *Bcmo1*<sup>-/-</sup> mice, in which BC accumulation was readily evidenced by an orange coloring of the fat depots (not shown). Serum retinol levels were similar regardless of genotype or diet (Figure 1D). iWAT total retinol levels (free retinol plus retinyl ester) were increased upon the BC diet in WT but not in *Bcmo1*<sup>-/-</sup> mice (Figure 1F). In *Bcmo1*<sup>-/-</sup> mice supplemented with BC, a compound that migrated shortly after all-*trans*-retinol with an absorption maximum of 402 nm was present (Fig. 1G). Spectral characteristics and retention time indicated that this compound is  $\beta$ -10'-apocarotenol, the corresponding alcohol of the primary *Bcdo2* cleavage product  $\beta$ -10'-apo-carotenal. To confirm this hypothesis, we used a  $\beta$ -10'-apocarotenol standard and reduced it to the corresponding alcohol by BH<sub>4</sub> treatment. In fact, this  $\beta$ -10'-apocarotenol standard had the same retention time and spectral characteristics of the compound that accumulated in *Bcmo1*<sup>-/-</sup> mice upon BC supplementation (Fig 2A and 2B). Finally, we confirmed the identity of this compound by tandem mass spectrometry as compared  $\beta$ -10'-apocarotenol standard substance (Fig. 2C-F). Thus, we concluded that in WT mice supplemented BC is largely converted to retinoids. When BC accumulated in *Bcmo1*<sup>-/-</sup> mice,

it is converted in part to  $\beta$ -10'-apocarotenal that is further reduced to the corresponding alcohol.

### Dietary BC reduces adiposity in WT mice

*Bcmo1*<sup>-/-</sup> mice had a lower average body weight than WT mice at the beginning of the study (17.3±0.4 g versus 18.5±0.2 g; p<0.05 Student's t test) and showed a tendency of higher body weight gain over the 14 week experimental period (Figure 3A). Body weight at the end of the study was comparable in all groups (data not shown). Cumulative energy intake over the 14 week experimental period was significantly higher in mice fed the BC diet than in those fed the control diet, and in *Bcmo1*<sup>-/-</sup> mice as compared to WT mice (Figure 3B). Energy efficiency (body weight gained per energy eaten) was similar among groups (Figure 3C). Even though BC supplementation did not affect final body weight in either genotype, it significantly decreased the percentage of body fat (by 28%, p<0.01) in WT but not in *Bcmo1*<sup>-/-</sup> mice (Figure 3D). In WT mice, reduction of depot mass after BC diet was evident for all three WAT depots examined (inguinal, gonadal and retroperitoneal) (Figure 3E); no such effect of BC on fat depots was observed in the *Bcmo1*<sup>-/-</sup> mice. Leptin levels in serum reflected changes in body adiposity, being reduced following dietary BC supplementation in the WT mice but not in the *Bcmo1*<sup>-/-</sup> mice (Table 1). There was a direct, positive correlation between serum leptin levels and iWAT mass (r = 0.617, p<0.001). Morphometric analysis showed that the mean sectional area of unilocular iWAT adipocytes was reduced after dietary BC supplementation in the WT mice (Figure 3F and 3G). Mean iWAT adipocyte area was similar in the two genotype groups after the control diet, but significantly higher in the *Bcmo1*<sup>-/-</sup> mice after the BC diet. Circulating levels of insulin, glucose and triacylglycerol were unaffected by diet or genotype (Table 1).

### Dietary BC results in a general down-regulation of gene expression in adipose tissue of WT mice

To analyze the effects of BC supplementation on transcriptional activities in adipose tissue in different genotypes we performed genome-wide expression analysis of iWAT of all individual animals. Principal component analysis of microarray results revealed a different gene expression signature in WT and *Bcmo1*-null mice, and a clear effect of dietary BC supplementation that changed the overall gene expression signature in the WT mice, but not in the *Bcmo1*-null mice (Figure 4A). From the 25139 spots with signal intensities above two times the background, 1597 positive spots were differentially expressed due to BC supplementation in the WT mice and only 84 in the *Bcmo1*-null mice (p<0.01) (Figure 4B). These 84 positive spots correspond to 81 genes, that are given in Table S1 and are likely regulated by BC or  $\beta$ -10'-apocarotenoid accumulation. None of the genes affected by BC supplementation in the WT mice (p<0.01) were affected in the *Bcmo1*-null mice (Figure 4B, 0 genes overlapping). In the WT mice, genes significantly regulated (p<0.01) by BC supplementation appeared to differ most in expression as compared to the other three groups; WT control diet, *Bcmo1*<sup>-/-</sup> control diet and *Bcmo1*<sup>-/-</sup> BC diet (Figure 4D). Remarkably, upon BC supplementation, 87% of the genes affected in WT mice were found to be down-regulated (Figures 4C and 4D). Pathway analysis using Metacore showed that genes encoding components of lipid and glucose metabolism-related pathways (including cholesterol biosynthesis, fatty acid metabolism, glycerophospholipid metabolism, pentose phosphate pathway, pyruvate metabolism and glycolysis/ gluconeogenesis) as well as ATP synthesis and oxidative phosphorylation were among the most affected

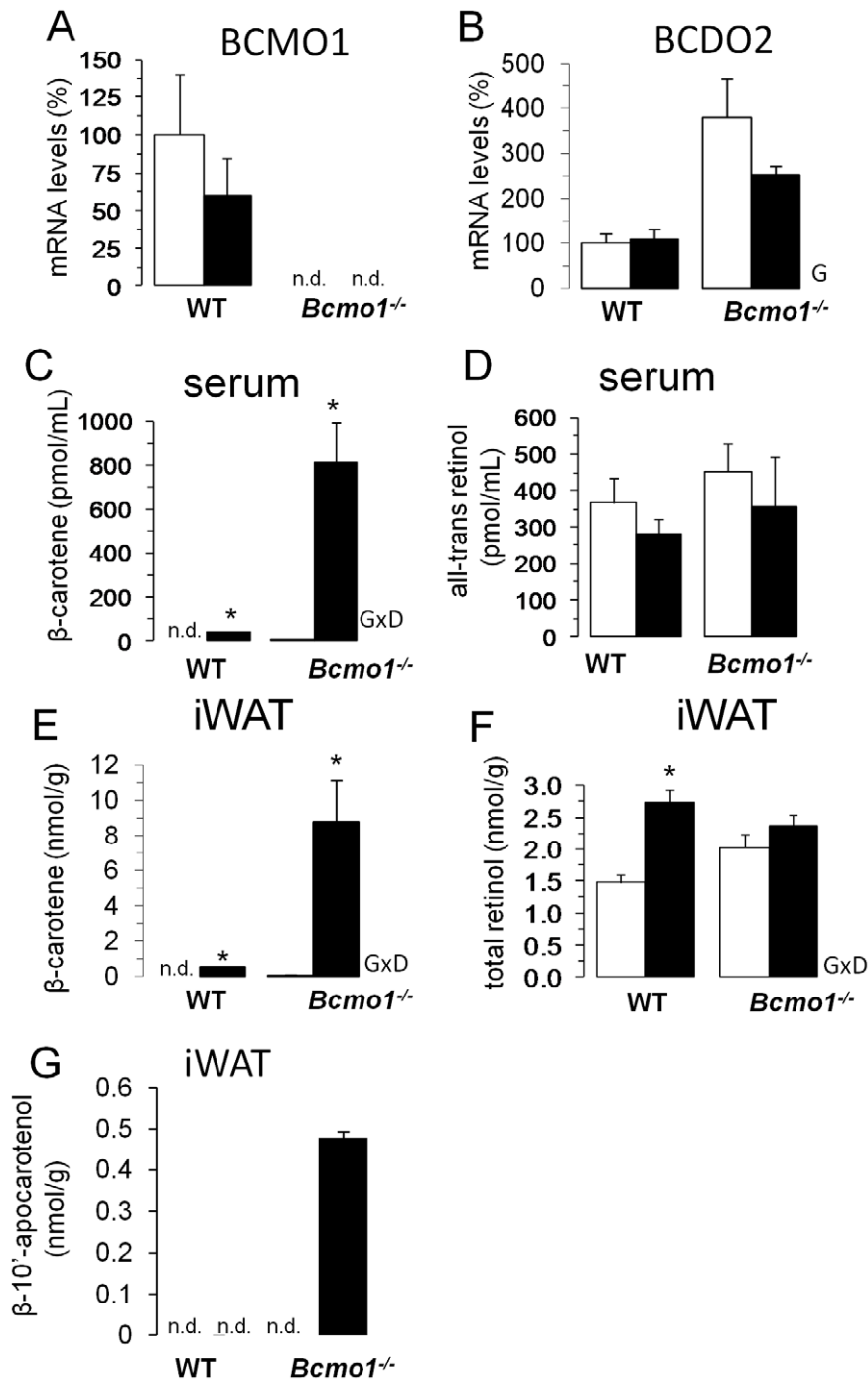


**Figure 1. Serum and inguinal white adipose tissue levels of β-carotene, retinoids and apocarotenoids.** (A, B) β-carotene -15, 15'-monooxygenase (*Bcmo1*) and β-carotene 9', 10'-dioxygenase (*Bcdo2*) mRNA levels in inguinal white adipose tissue (iWAT) of wild-type (WT) and *Bcmo1*-null (*Bcmo1*<sup>-/-</sup>) mice after 14 weeks on a control diet (open bars) or a β-carotene-enriched diet (black bars). Quantitative real-time PCR was used to determine normalized gene expression levels. (C-G) β-carotene, retinol and 10' β-apocarotenol levels in serum and iWAT of WT and *Bcmo1*<sup>-/-</sup> mice after 14 weeks on a control diet (open bars) or a β-carotene-enriched diet (black bars). β-carotene, retinol and β-10'-apocarotenol were determined by HPLC (see Materials and Methods). Total retinol refers to free retinol plus retinyl esters. Data in (A to G) are the mean ± SEM of 6 animals per group; n.d. non-detectable; GxD, interaction between genotype and diet in two-way ANOVA analysis ( $p < 0.05$ ); G, genotype effect in two-way ANOVA analysis ( $p < 0.05$ ); \*,  $p < 0.05$  in Student's *t* test, BC diet versus control diet. doi:10.1371/journal.pone.0020644.g001

(Table S2). Because of the close connections between neovascularisation and adipose tissue expansion [34–35], we specifically examined changes in the expression of angiogenesis-related

genes. As expected, BC supplementation triggered a generalized down-regulation of these genes in the WT mice, but not in the *Bcmo1*<sup>-/-</sup> mice (Table S3).

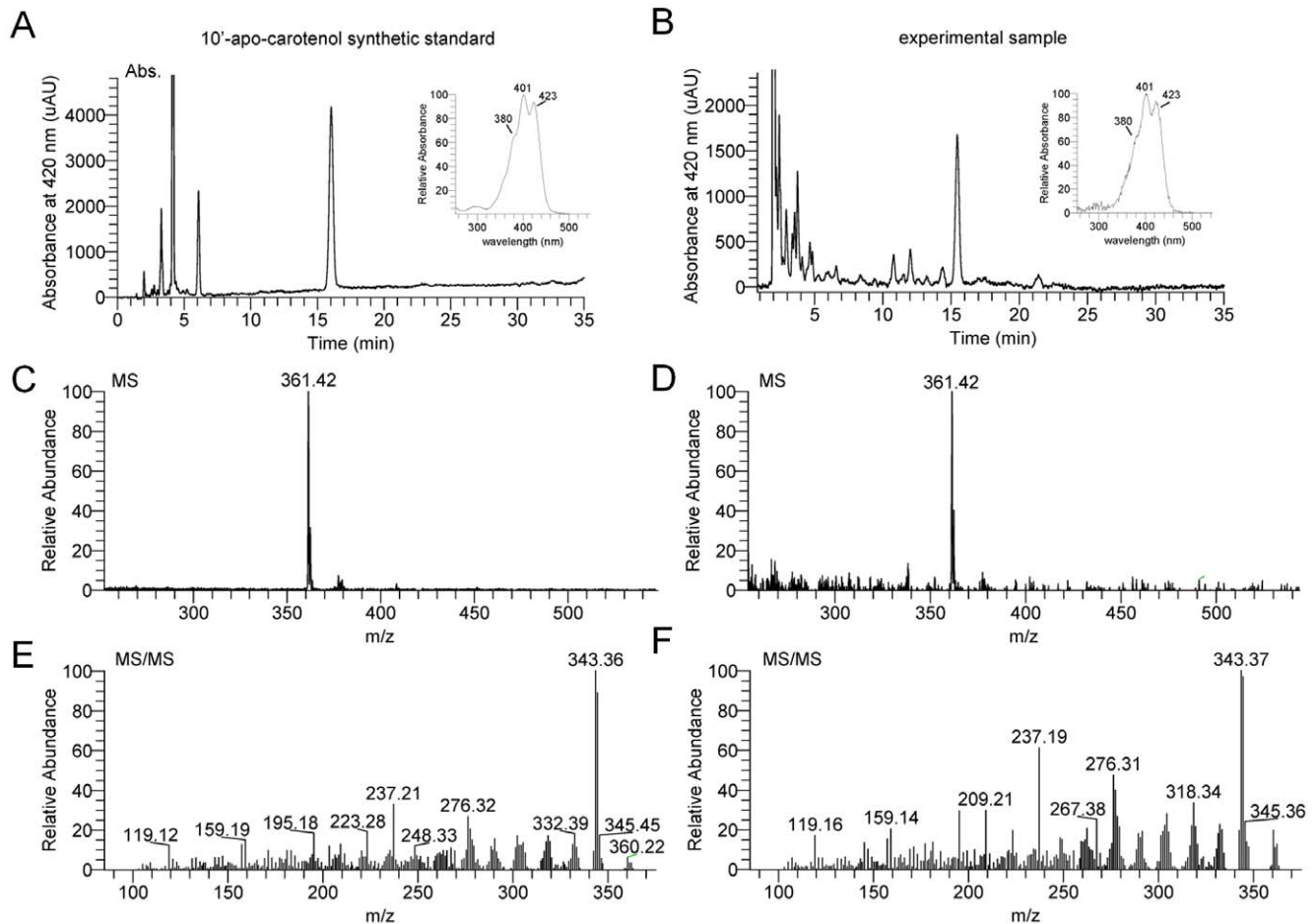


**Figure 2.  $\beta$ -10'-apocarotenol is the major  $\beta$ -carotene cleavage product in *Bcmo1*<sup>-/-</sup> mice.** HPLC-profile at 420 nm of (A) the synthetic  $\beta$ -10'-apocarotenol standard and (B) a lipid extract of iWAT of BC supplemented *Bcmo1*<sup>-/-</sup> mice. Insets show the spectral characteristics of the  $\beta$ -10'-apocarotenol standard (peak 1) as compared to peak 1'. (C, D) Single extracted ion chromatograms for  $\beta$ -10'-apocarotenol standard ( $m/z = 361.42$ ; peak 1 and 1'). (E, F) Fragmentation pattern of a parent ion selected at  $m/z = 361.42$  are identical for the  $\beta$ -10'-apocarotenol standard (peak 1) and peak 1'.

doi:10.1371/journal.pone.0020644.g002

### Dietary BC down-regulates PPAR $\gamma$ and PPAR $\gamma$ target genes in adipose tissue of WT mice

A general effect of BC supplementation in reducing global transcriptional activity in iWAT of WT mice suggested that the activity of a master control transcription factor of adipose tissue biology was affected. In this context, a batch promoter analysis with Eldorado coupled to matinspector (Genomatix Suite) revealed that 54% of the top 50 down-regulated genes in iWAT of BC supplemented WT mice harbored a putative PPAR response element in their promoter region ( $p$  value:  $1.33e^{-6}$ ) with at least 85% homology with the matrix similarity defined by Genomatix (Table 2). Interestingly, the same kind of analysis in iWAT of BC supplemented *Bcmo1*<sup>-/-</sup> mice revealed that the presence of putative PPAR responsive element was not significant ( $p$  value: 0.81). Microarray results indicated that iWAT gene expression of PPAR $\gamma$  and its heterodimeric partner RXR $\alpha$  were significantly decreased following BC supplementation in the WT mice ( $-1.75$  and  $-1.57$  fold-change, respectively,  $p < 0.05$ ), but not in the *Bcmo1*<sup>-/-</sup> mice. Q-PCR analysis confirmed the microarray results and thus down-regulation of the mRNA expression levels of PPAR $\gamma$  and RXR $\alpha$  after BC supplementation in iWAT of WT mice, but not of *Bcmo1*<sup>-/-</sup> mice (Figure 5A and 5B). Additionally, PPAR $\gamma$  protein expression levels in iWAT

followed the same pattern as the mRNA levels, as indicated by immunoblotting results (Figure 5D). In contrast, iWAT mRNA levels of CYP26a1, a retinoic acid hydroxylase that is transcriptionally induced by retinoic acid in a strictly RAR-dependent manner [36;37], were increased by 138% after BC supplementation in the WT mice, but not in the *Bcmo1*<sup>-/-</sup> mice (Figure 5E), suggesting a *Bcmo1*-dependent enhancement of retinoic acid signalling in iWAT following chronic BC supplementation. Finally, to provide direct evidence for down-regulation of PPAR $\gamma$  activity after BC supplementation in the WT mice, we determined iWAT mRNA levels of LPL, a well-known target of PPAR $\gamma$ :RXR $\alpha$ , by Q-RT-PCR. As shown in Fig. 5C, LPL mRNA levels were significantly decreased in WT mice upon BC supplementation. Changes in gene expression of PPAR $\gamma$ , RXR $\alpha$  and LPL in the gonadal fat depot followed the same pattern as in the inguinal depot (Figure S1).

### Discussion

Here we analyzed the effects of dietary BC on whole-body adiposity and adipose tissue physiology. We supplemented WT and *Bcmo1*<sup>-/-</sup> mice with BC and compared them to non-supplemented littermates. Our results revealed a *Bcmo1*-dependent, adiposity reducing effect of BC supplementation, as percent

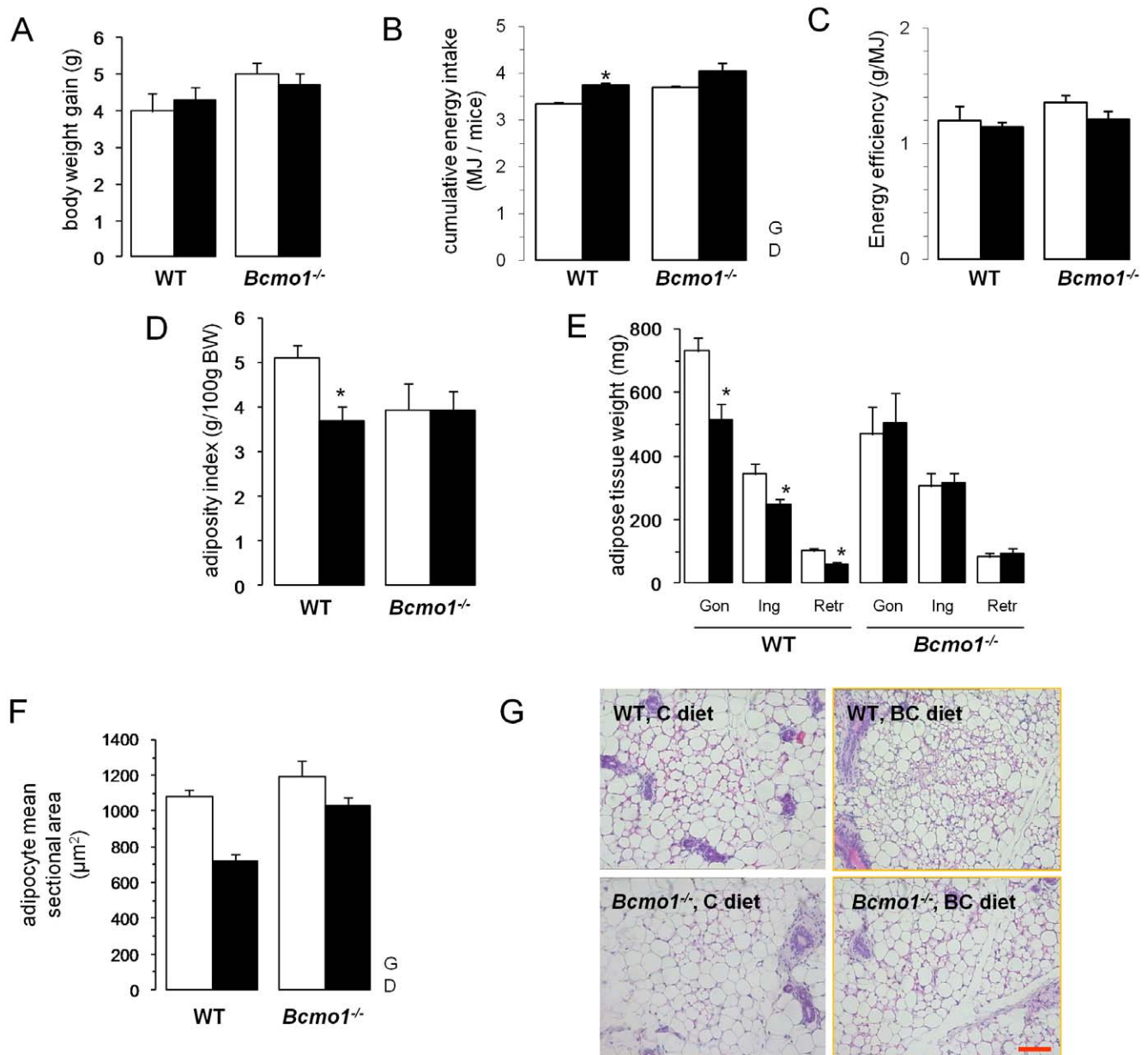


**Figure 3. Supplementation of  $\beta$ -carotene alters body adiposity in wild-type mice.** (A) Effects of dietary  $\beta$ -carotene supplementation on body weight gain, (B) cumulative energy intake, (C) energy efficiency, (D) adiposity index, (E) adipose depot weight, and (F) inguinal adipocyte mean sectional area, in wild-type (WT) and *Bcmo1*-null (*Bcmo1*<sup>-/-</sup>) mice. In (G), micrographs of sections of inguinal fat in the four groups are shown (The scale bar gives 100  $\mu$ m). Data in (A to E) are the mean  $\pm$  SEM of 6 animals per group, and data in (F) of 3 animals per group. Open bars, animals on the control diet; black bars, animals on the  $\beta$ -carotene-enriched diet. Body weight gain, cumulative energy intake and energy efficiency over the entire 14 week experimental period are shown. Adiposity index corresponds to the sum of all entirely dissected white adipose tissue depots (gonadal, Gon; inguinal, Ing; and retroperitoneal, Retr), expressed as percentage of the animal body weight (BW). G, genotype effect in two-way ANOVA analysis ( $p < 0.05$ ); D, effect of diet in two-way ANOVA analysis ( $p < 0.05$ ); \*,  $p < 0.05$  in Student's *t* test, BC diet versus control diet. doi:10.1371/journal.pone.0020644.g003

body fat, adipose depot mass, iWAT adipocyte size and leptin serum levels were all significantly reduced after BC supplementation in the WT mice, but not in the *Bcmo1*<sup>-/-</sup> mice (Figure 3). Reduced adiposity in WT mice after BC supplementation was not associated with adverse effects on blood parameters measured such as increased circulating triacylglycerol levels. Moreover, no harmful effects of BC supplementation on parameters such as body weight gain, food intake, or lung tissue histology were observed in the animals (this work and [38]). Although relatively low dietary vitamin A was fed, blood retinol levels were well

maintained and within the expected range for adult mice in the different genotypes and supplementation groups (Figure 1D). Additionally, stored retinol was found in the adipose tissue (Figure 1F) and in the liver (data not shown), indicating no gross changes in vitamin A homeostasis in animals of different supplementation groups.

Microarray analyses revealed that BC supplementation altered the overall iWAT gene expression signature in WT mice but not in *Bcmo1*<sup>-/-</sup> mice. Strikingly, none of the genes altered in its expression levels upon BC supplementation in the WT mice



**Table 1.** Fed blood parameters in wild-type and *Bcmo1*<sup>-/-</sup> mice following control and  $\beta$ -carotene enriched diet.

	WT control diet	WT BC diet	<i>Bcmo1</i> <sup>-/-</sup> control diet	<i>Bcmo1</i> <sup>-/-</sup> BC diet	Anova
Glucose (mg/dL)	211 $\pm$ 22	220 $\pm$ 9	242 $\pm$ 12	248 $\pm$ 21	
Triacylglycerol (mg/mL)	0.31 $\pm$ 0.05	0.30 $\pm$ 0.03	0.31 $\pm$ 0.05	0.40 $\pm$ 0.08	
Insulin (ng/mL)	0.47 $\pm$ 0.20	0.36 $\pm$ 0.10	0.49 $\pm$ 0.15	0.59 $\pm$ 0.18	
Leptin (ng/mL)	9.63 $\pm$ 1.69	4.09 $\pm$ 0.59*	6.72 $\pm$ 1.74	7.33 $\pm$ 1.59	GxD

Analysis were carried out in wild-type (WT) and *Bcmo1*<sup>-/-</sup> female mice fed for 14 weeks a control diet or a  $\beta$ -carotene-enriched diet (BC diet), starting at 5 weeks of age. Data are the mean  $\pm$  SEM of 6 animals per group. \*,  $p < 0.05$  in Student's t test, BC diet versus control diet; GxD, interaction between genotype and diet in two-way ANOVA analysis ( $p < 0.05$ ).

doi:10.1371/journal.pone.0020644.t001

( $p < 0.01$ ) was changed in *Bcmo1* knockout mice (Figure 4). BC supplementation led to a general down-regulation of gene expression in iWAT of WT mice. This finding indicated that the

activity of major transcriptional regulator of iWAT was affected by BC supplementation. Microarray, Q-PCR and immunoblotting analysis consistently confirmed a reduction of PPAR $\gamma$  expression

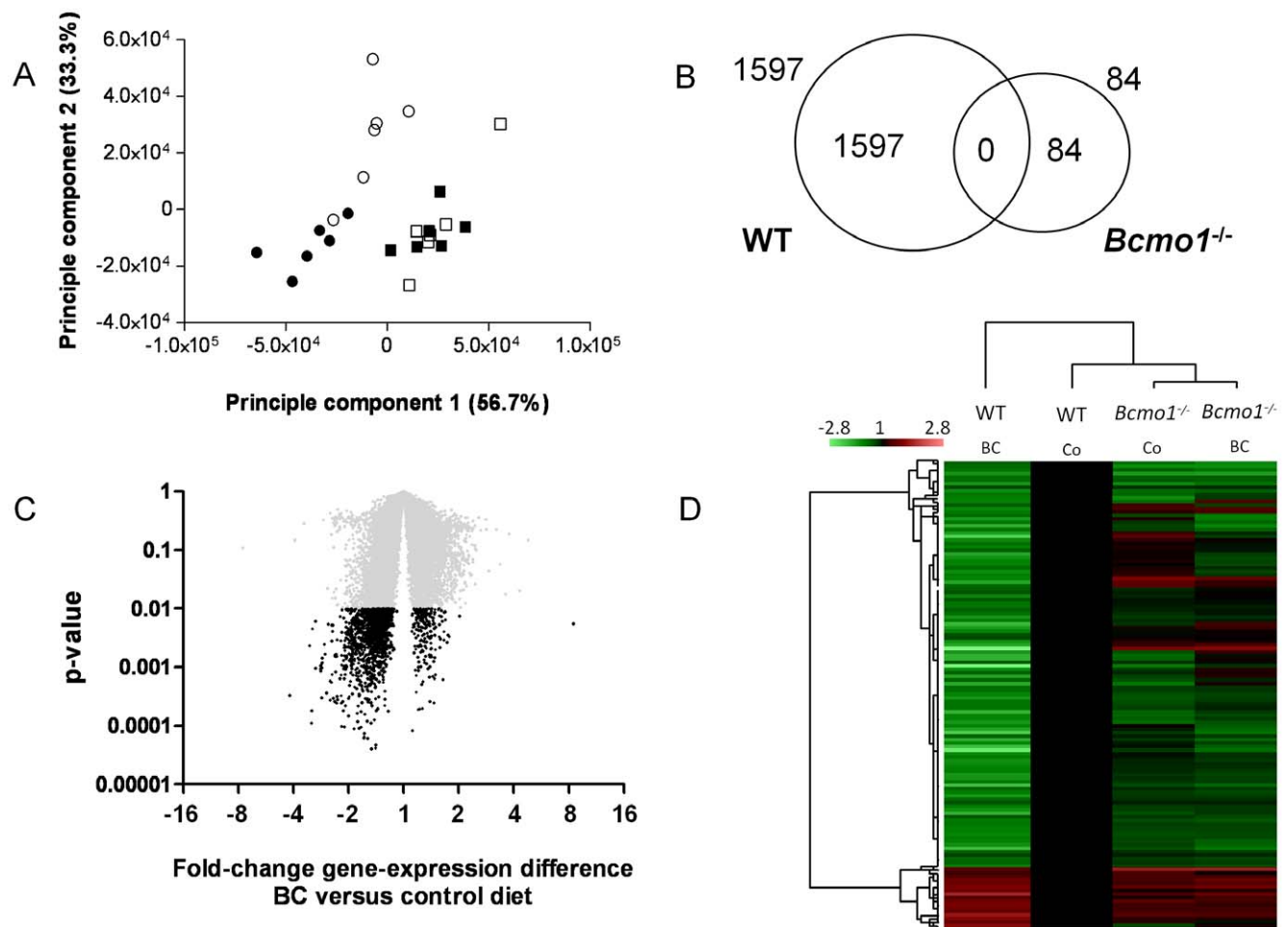


**Figure 4. Supplemental analysis of gene expression profiles in wild-type but not in *Bcmo1*<sup>-/-</sup> mice.** (A) Principal component analysis of transcriptional profiles in inguinal white adipose tissue of female wild-type (circles) and *Bcmo1*<sup>-/-</sup> (squares) mice fed the control diet (open symbols) or the  $\beta$ -carotene diet (closed symbols). Genome-wide expression profiles were obtained using the 4 $\times$ 44 k Agilent whole mouse genome microarrays for each animal in the experiment ( $n = 6$  per group). (B) Venn diagram representing the number of significantly regulated genes ( $p < 0.01$ ) due to BC supplementation in wild-type (WT) and in *Bcmo1*-null (*Bcmo1*<sup>-/-</sup>) mice and the number of significantly regulated genes regardless of genotype (overlap). (C) Volcano plot representing the effect of BC supplementation on gene expression in WT mice, with the fold-change on the x-axis and the corresponding Student's t-test p-value on the y-axis. Every spot is a single gene and in black are all genes with a p-value  $< 0.01$ . (D) Heat map representing the expression level of all genes regulated by BC with a Student's t-test  $p < 0.01$  in the WT mice in all four groups; WT control (Co) diet, WT BC diet, *Bcmo1*<sup>-/-</sup> control diet and *Bcmo1*<sup>-/-</sup> BC diet. Relative expression of every single gene was compared to gene expression in WT mice on the control diet and consequently, gene expression of every single gene in WT mice on the control diet was set to 1.0.

doi:10.1371/journal.pone.0020644.g004

**Table 2.** Batch promoter analysis focused on peroxisome proliferator-activated receptor (PPAR) of the fifty top down-regulated genes in inguinal white adipose tissue of wild-type mice after  $\beta$ -carotene supplementation.

Gene	Gene name	p value	fold-change	putative PPRE
Npr3	natriuretic peptide receptor 3	0.00033	-4.18	Yes
Mosc1	MOCO sulphurase C-terminal domain containing 1	0.00234	-3.26	Yes
Dnmt3l	DNA (cytosine-5-)-methyltransferase 3-like	0.00452	-3.14	
Scd2	stearoyl-Coenzyme A desaturase 2	0.00606	-3.02	Yes
Lep	Leptin	0.00106	-2.84	
Rbp4	retinol binding protein 4, plasma	0.00030	-2.80	Yes
Pnpla3	patatin-like phospholipase domain containing 3	0.00098	-2.78	
Dgat2	diacylglycerol O-acyltransferase 2	0.00166	-2.68	Yes
Slc2a5	solute carrier family 2 (facilitated glucose transporter), member 5	0.02198	-2.60	
Fads3	fatty acid desaturase 3	0.00027	-2.52	Yes
Alb1	albumin 1	0.00058	-2.51	Yes
Mod1	malic enzyme, supernatant	0.00280	-2.46	Yes
Gsta3	glutathione S-transferase, alpha 3	0.00075	-2.46	
Mogat2	monoacylglycerol O-acyltransferase 2	0.00408	-2.44	Yes
Fabp5	fatty acid binding protein 5, epidermal	0.00026	-2.37	
Elovl6	ELOVL family member 6, elongation of long chain fatty acids (yeast)	0.01515	-2.36	Yes
Ela1	elastase 1, pancreatic	0.00155	-2.35	Yes
Cav1	caveolin, caveolae protein 1	0.00083	-2.35	
Cspg3	chondroitin sulfate proteoglycan 3	0.02156	-2.33	
Apol6	apolipoprotein L, 6	0.00167	-2.33	Yes
LOC676546	similar to monocyte to macrophage differentiation-associated	0.00024	-2.32	Yes
Sncg	synuclein, gamma	0.00155	-2.32	
Ppp2r5b	protein phosphatase 2, regulatory subunit B (B56), beta isoform	0.00294	-2.31	
Tkt	Transketolase	0.01153	-2.31	
Ntsr2	neurotensin receptor 2	0.00032	-2.31	Yes
Acss2	acyl-CoA synthetase short-chain family member 2	0.01181	-2.28	Yes
Mid1ip1	Mid1 interacting protein 1 (gastrulation specific G12-like (zebrafish))	0.03037	-2.21	Yes
Retn	Resistin	0.00282	-2.19	
Lpgat1	lysophosphatidylglycerol acyltransferase 1	0.00024	-2.19	Yes
Lct1	lactase-like	0.00010	-2.18	Yes
Slc6a13	solute carrier family 6 (neurotransmitter transporter, GABA), member 13	0.00394	-2.17	
Comt	catechol-O-methyltransferase	0.00946	-2.17	
Thbd	Thrombomodulin	0.01020	-2.17	Yes
Orm2	orosomucoid 2	0.00026	-2.14	Yes
Orm1	orosomucoid 1	0.00018	-2.13	Yes
Lrrc39	leucine rich repeat containing 39	0.00130	-2.12	
Sc5d	sterol-C5-desaturase (fungal ERG3, delta-5-desaturase) homolog ( <i>S. cerevisiae</i> )	0.00095	-2.12	
Fabp4	fatty acid binding protein 4, adipocyte	0.00690	-2.11	Yes
Lss	lanosterol synthase	0.00103	-2.10	
Odz4	odd Oz/ten-m homolog 4 ( <i>Drosophila</i> )	0.00063	-2.10	
Slc9a2	solute carrier family 9 (sodium/hydrogen exchanger), member 2	0.00214	-2.10	Yes
Aldh1a7	aldehyde dehydrogenase family 1, subfamily A7	0.00010	-2.10	Yes
Cpa2	carboxypeptidase A2, pancreatic	0.00157	-2.10	
Timp4	tissue inhibitor of metalloproteinase 4	0.01792	-2.09	
Slc2a4	solute carrier family 2 (facilitated glucose transporter), member 4	0.01228	-2.09	Yes
Adamts5	a disintegrin-like and metallopeptidase (reprolysin type) with thrombospondin type 1 motif, 5 (aggrecanase-2)	0.00287	-2.08	
Kcnj14	potassium inwardly-rectifying channel, subfamily J, member 14	0.00022	-2.07	
Slc16a12	solute carrier family 16 (monocarboxylic acid transporters), member 12	0.00221	-2.07	Yes

**Table 2.** Cont.

Gene	Gene name	p value	fold-change	putative PPRE
Dbi	diazepam binding inhibitor	0.00384	-2.06	Yes
Fasn	fatty acid synthase	0.00220	-2.06	

Batch promoter analysis was performed with Eldorado coupled to matinspector (Genomatix Suite). Yes in the right column indicates the presence in the corresponding gene promoter of a putative PPAR response element (PPRE) with at least 85% homology with the matrix similarity defined by Genomatix.  
doi:10.1371/journal.pone.0020644.t002

(Figure 5A and 5D). *In silico* analysis of the promoter regions of the top 50 BC down-regulated genes in wild-type mice showed that more than 50% contained a PPAR response element (Table 2). The p value associated ( $1.33e^{-6}$ ) strongly supported the importance of PPAR $\gamma$  within this gene set, since it represents the probability to obtain an equal or greater number of sequences with

a match in a randomly list of genes. Interestingly, such result was not reproduced in the *Bcmo1*<sup>-/-</sup> mice (p value 0.81; not significant) underlying the key role of this enzyme in the repression of PPAR $\gamma$  activity by BC. Thus, the reduction of PPAR $\gamma$  activity and the down-regulation of its target genes likely explain the reduced adiposity of WT mice upon BC supplementation.

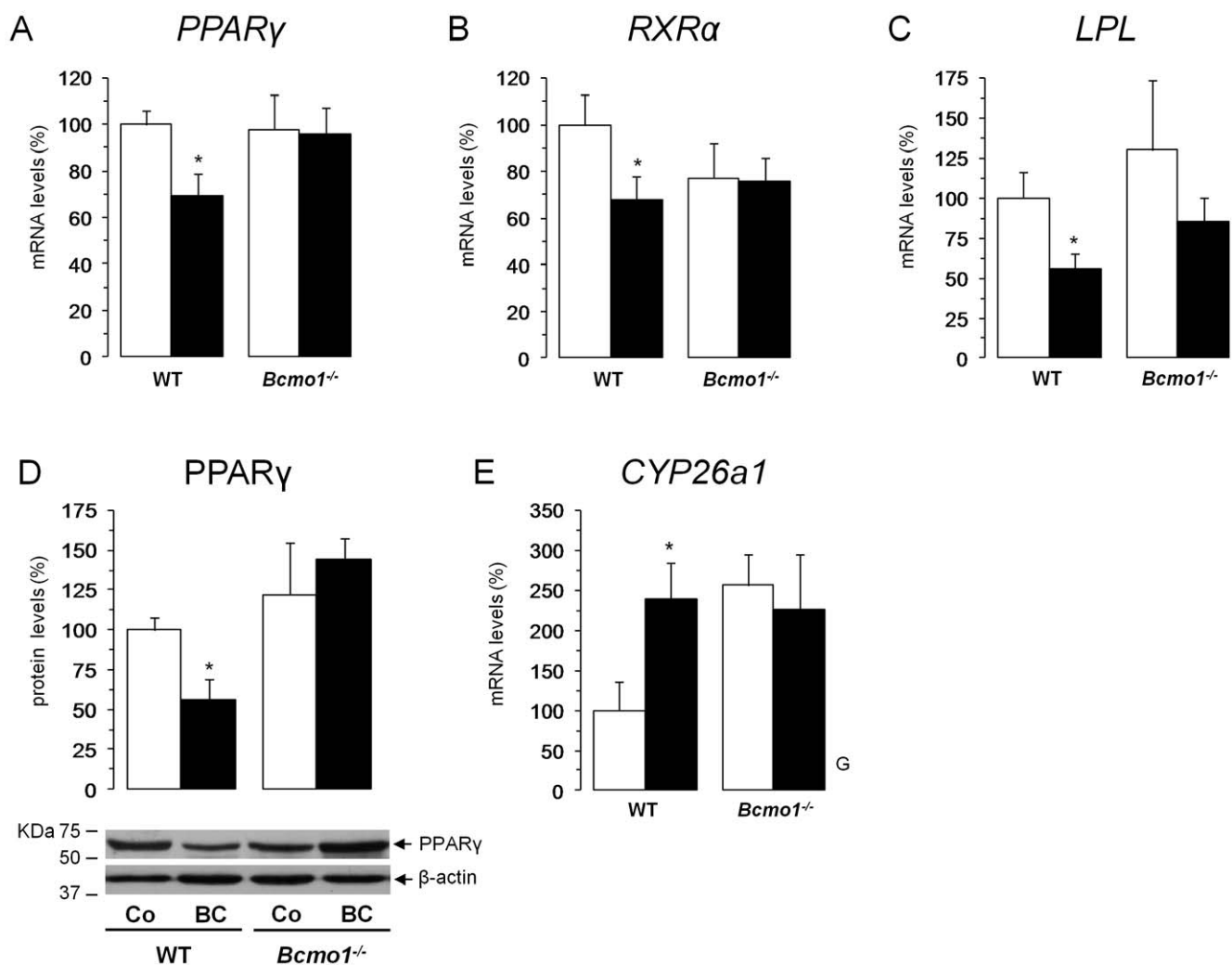


**Figure 5.  $\beta$ -carotene supplementation reduces PPAR $\gamma$  expression both on the mRNA and protein level.** (A) PPAR $\gamma$  mRNA levels, (B) RXR $\alpha$  mRNA levels, (C) lipoprotein lipase (LPL) mRNA levels, (D) PPAR $\gamma$  protein levels and (E) *Cyp26a1* mRNA levels in inguinal white adipose tissue of wild-type (WT) and *Bcmo1*-null (*Bcmo1*<sup>-/-</sup>) mice after 14 weeks on a control diet (open bars) or a  $\beta$ -carotene -enriched diet (black bars). Quantitative real-time PCR was used to determine normalized gene expression levels as described in Materials and Methods. Immunoblotting was used to determine expression levels of PPAR $\gamma$  and  $\beta$ -actin, which was used as internal control for equal loading and blotting; shown at the bottom of (D) is a representative immunoblot for the two proteins. Data in (A to E) are the mean  $\pm$  SEM of 6 animals per group. G, effect of genotype in two-way ANOVA analysis (p<0.05); \*, p<0.05 in Student's t test, BC diet versus control diet.  
doi:10.1371/journal.pone.0020644.g005



Centric cleavage of BC by *Bcmo1* leads to retinaldehyde production which can be converted to retinol and retinyl ester for storage and to retinoic acid. Enzymes catalyzing these reactions are expressed in adipocytes [7;16]. Retinoids such as retinoic acid and retinaldehyde are ligands for nuclear receptors including RARs and PPARs that help control adipogenesis and adipocyte metabolism. Treatment with retinoic acid has been shown to inhibit differentiation of pre-adipose cells in culture by blocking PPAR $\gamma$  induction in an RAR-mediated manner [18;39], and to result *in vivo* in mice in reduced PPAR $\gamma$  expression levels in WAT [19] and reduced whole body adiposity [19;31]. Moreover, a recent study showed that BC, but not retinol, decreases PPAR $\gamma$  and reduces lipid storage capacity in mature white adipocytes in culture [15]. This effect involves production of retinoic acid from BC, is blocked by a *Bcmo1* chemical inhibitor (fenretinide), and is dependent on RARs [15]. Importantly, BC was accumulated following BC diet in serum and tissues of WT mice (Figure 1C and 1E), suggesting that not all BC undergoes intestinal cleavage in WT mice. Thus, an adipose tissue-specific, *Bcmo1*-dependent production of retinoids, such as retinoic acid, from BC might explain the down-regulation of iWAT PPAR $\gamma$  expression levels and the overall changes in iWAT gene expression patterns and adiposity-related end-points observed in this work in WT mice following chronic exposure to a BC-enriched diet. The involvement of RAR-signalling is sustained by the *CYP26a1* gene-expression data showing increased expression of this retinoic acid target gene following BC supplementation selectively in the iWAT of WT mice (Figure 5E). Additionally, iWAT mRNA levels of some other genes for which there is evidence of transcriptional up-regulation or down-regulation in response to retinoic acid were significantly increased and decreased, respectively, following BC supplementation in the WT mice, but not in the *Bcmo1*-null mice (microarray data shown in Table S4), including leptin. Leptin expression has been shown to be decreased by retinoic acid [24–27] and blood levels of this adipokine were significantly reduced in WT mice supplemented with BC.

Interestingly, expression of the *Bcdo2* gene was up-regulated in iWAT of *Bcmo1*-null mice, both under control and BC diet (Figure 1B). In fact, relatively large amounts of  $\beta$ -10'-apocarotenol became detectable in WAT of *Bcmo1*<sup>-/-</sup> mice upon BC supplementation. This compound derives by the reduction of the primary BC cleavage product  $\beta$ -10'-apo-carotenal. It has been reported that apocarotenoids such as  $\beta$ -14-apo-carotenal can repress PPAR $\gamma$  - and RXR-mediated responses in cell culture [32]. However, we found not much evidence that apocarotenoid formation in *Bcmo1*<sup>-/-</sup> mice influenced adipocyte physiology. Our results indicate that the effects of BC on adipocyte biology are clearly dependent on *Bcmo1*, as those effects were not found in *Bcmo1*-deficient animals that express *Bcdo2*.

In summary, this study revealed a *Bcmo1*-dependent, adiposity reducing effect of long-term BC supplementation in mice. In this context, we provide evidence that BC-derived retinoids influence adipocyte physiology. *Bcmo1* is a PPAR $\gamma$  target gene [13], and our analysis indicates that the *Bcmo1*-dependent, adiposity-reducing effect of BC is mediated by a reduction of PPAR $\gamma$  activity in adipocytes. Thus, our findings establish *Bcmo1* as key component for the crosstalk between RAR- and PPAR $\gamma$ -signaling pathways in the control of body adiposity.

Our results may also have implications in the context of the current obesity pandemics. There is evidence of an impact of BC and vitamin A status on parameters related to adiposity in humans [40]. Circulating BC levels are inversely correlated with risk of human type 2 diabetes, a pathology associated with obesity [41–44]. Additionally, reduced plasma levels of carotenoids, including

BC, are commonly found in obese children [45]. Genetic polymorphisms in the *Bcmo1* gene have been described that alter the activity of the encoded human protein [46;47]. Our work suggests that BC intake may have different consequences on body adiposity in subjects carrying different *Bcmo1* functional gene variants. Thus, the involvement of BC and *Bcmo1* in human obesity deserves further research.

## Materials and Methods

### Animals and diets

The animal experiment was conducted according to accepted standards of humane care and use of laboratory animals, and was approved by the bioethical committee of the University of Freiburg (Az.: 35/9185.81/G-07/30). C57/BL6;129Svj-*Bcmo1*<sup>tm1Dnp</sup> (*Bcmo1*<sup>-/-</sup>) mice previously described by Hessel et al. [7] and mixed background F1 generation of C57/BL6;129Svj mice as WT controls were used. During the breeding and weaning periods and up to 5 weeks of age all mice were maintained on breeder chow containing 14000 IU vitamin A/kg diet (Provimi Kliba AG, Kaiseraugst, Switzerland). Five-week-old WT and *Bcmo1*<sup>-/-</sup> female mice were fed a defined, pelletized diet containing 1500 IU vitamin A/kg and 10% energy as fat, with (BC diet) or without (control diet) 150 mg BC/kg diet (n = 6 animals per group) for 14 weeks, after which they were euthanized. Detailed composition of these diets is shown in Table 3. A relatively low dose of dietary vitamin A was used to maximize intestinal BC absorption, which can be repressed by preformed vitamin A [48]. The dose used was previously shown to be sufficient to maintain vitamin A homeostasis while allowing tissue BC accumulation both in WT and *Bcmo1*<sup>-/-</sup> mice [9]. The experimental diets were prepared by Research Diets, Inc (New Brunswick, NJ, USA) by cold extrusion so as to protect BC from heat treatment and incorporating a water-soluble formulation in the form of beadlets containing BC, DL- $\alpha$ -tocopherol, ascorbyl palmitate, corn oil, fish gelatin, sucrose and corn starch. The control diet contained control beadlets devoid of BC, but with all other ingredients. All beadlets were kindly provided by DSM Nutritional Products Ltd (Basel, Switzerland). Mice were maintained under environmentally controlled conditions (24°C, 12 h/12 h light/dark cycle) in groups of 3 animals per cage and with *ad libitum* access to feed and water. Body weight and food intake were determined twice per week (3 and 4 days intervals). Energy intake was estimated on a per-cage basis from the actual amount of food consumed by the animals and its caloric equivalence (16 MJ/kg for both control and BC diet). On the day of the necropsy, the animals were sacrificed according to the animal protocol of the University of Freiburg (Germany). First, animals were subjected to inhalation of isofluran. Then, 100–150 mg/kg KGW Ketamin (Ketamin 10%, Essex) and 5–10 mg/kg KGW Xylazin (Rompun 2 %, Bayer) were injected intraperitoneally. Blood was drawn from the vena cava, and animals were then sacrificed by cervical dislocation. Inguinal (iWAT), gonadal (periovarian) and retroperitoneal white adipose tissue (WAT) depots were excised in their entirety according to Cinti [49], weighed, snap-frozen in liquid nitrogen and stored at -80°C until analysis. The continuous subcutaneous fat depot comprising the dorsolumbar and inguinal areas was taken as iWAT. The combined mass of all WAT pads taken expressed as a percentage of body weight was used as adiposity index. For three animals in each group, one entire iWAT lobule was fixed for histological studies.

### Histology and immunohistochemistry

Entire iWAT lobules were fixed by immersion in the perfusion fixative (4% paraformaldehyde in 0.1 M sodium phosphate buffer, pH 7.4) overnight at 4°C, dehydrated, cleared and then paraffin-

**Table 3.** Composition of the control and beta-carotene (BC) diets.

	Control diet	BC diet
<b>Macronutrients</b>		
Protein (g/100 g)	19.2	19.2
Carbohydrate (g/100 g)	67.2	67.2
Fat (g/100 g)	4.3	4.3
Kcal/g (MJ/kg)	3.84 (16)	3.84 (16)
Calories from protein (%)	20	20
Calories from carbohydrate (%)	70	70
Calories from fat (%)	10	10
<b>Ingredients (g/Kg)</b>		
Casein, 30 mesh	189	189
L-Cystine	2.8	2.8
Corn Starch	298	298
Maltodextrin 10	33	33
Sucrose	331	331
Cellulose, BW200	47	47
Soybean Oil	24	24
Lard	19	19
Salt Mix, S10026	9.5	9.5
DiCalcium Phosphate	12	12
Calcium Carbonate	5.2	5.2
Potassium Citrate, 1 H <sub>2</sub> O	16	16
Vitamin Mix V13001 with no added vitamin A	9.5	9.5
Vitamin A (retinol acetate, 500,000 IU/g)	0.003	0.003
Choline bitartrate	1.9	1.9
BC beadlets with 100 mg BC/g*	0	1.5
Control beadlets without BC	1.5	0
FD&C Yellow Dye #5	0	0.024
FD&C Red Dye #40	0.047	0
FD&C Blue Dye #1	0	0.024

BC beadlets contained BC, DL- $\alpha$ -tocopherol, ascorbyl palmitate, corn oil, fish gelatin, sucrose and corn starch. Control beadlets were devoid of BC, but with all other ingredients. All beadlets were kindly provided by DSM Nutritional Products Ltd (Basel, Switzerland). The experimental diets were prepared by Research Diets, Inc (New Brunswick, NJ, USA) by cold extrusion so as to protect BC from heat treatment.

doi:10.1371/journal.pone.0020644.t003

embedded so that the plane of section corresponded with the one of the wider surface. 3  $\mu$ m-thick sections at the same level were obtained and stained with hematoxylin/eosin for morphometric analysis, performed by digital acquisition of adipose tissue areas (Digital Still Camera DXM 1200 and NIKON 6000 Eclipse Microscope). Two histological sections were counted per mouse.

### Serum parameters

Commercial enzymatic colorimetric kits were used for the determination of circulating levels of triacylglycerol (Triglyceride (INT) 20, Sigma Diagnostics, St Louis, MO, USA) and glucose (D-Glucose UV-method, Roche Biopharm GmbH, Darmstadt, Germany). Serum levels of leptin and insulin were measured as described before [50] with some minor differences. Briefly, sera were diluted 4x in High Performance ELISA buffer (Sanquin, Amsterdam, The Netherlands) before adipokine analyses using the

mouse serum adipokine Lincoplex Kit (Linco Research, Nuclilab, Ede, The Netherlands). The assays were conducted according to the manufacturer's protocol and measured using the Bio-Plex (Bio-Rad, Venendaal, The Netherlands) system with Bio-Plex software. All individual samples were analyzed in duplicate and averaged.

### Analysis of retinoids, apocarotenoids, and carotenoids

Retinoids and carotenoids were extracted from serum under dim red safety light (600 nm) as described previously [7]. Adipose tissue (~40 mg) was incubated with 100  $\mu$ L of 12% pyrogallol in ethanol, 200  $\mu$ L of 30% KOH in water and 1 ml ethanol for 2 h at 37°C. After saponification, 1 ml H<sub>2</sub>O was added. The samples were extracted with 3 ml of ether/hexane (2:1, stabilized with 1% ethanol) twice, and diluted with 2 ml H<sub>2</sub>O and 2 ml ethanol. After centrifugation for 5 min at 800  $\times$  g, the organic layer was collected. The extract was evaporated in a Speedvac and dissolved in HPLC solvent. HPLC separation of carotenoids and retinoids and quantification of peak integrals was performed as described previously [6]. Solvents for HPLC and extraction were purchased in HPLC grade from Merck (Darmstadt, Germany).  $\beta$ -10'-apocarotenol was a gift of Dr. Hansgeorg Ernst (BASF, Germany). For  $\beta$ -10'-apocarotenol production, the standard was dissolved in 1 ml ethanol and reduced with BH<sub>4</sub> on ice. After 20 min, reaction products were extracted upon addition of 1 ml H<sub>2</sub>O with 1 ml hexanes. The organic phase was dried with a speedvac and redissolved in hexanes and subjected to HPLC analysis. The identity of  $\beta$ -10'-apocarotenol was further confirmed by LC/MS. The saponified lipophilic extract from iWAT was injected onto a Zorbax Sil column (Agilent Technologies, Santa Clara, CA) equilibrated with 90 % hexane and 10 % acetylacetate (v:v). The eluant was directed into LXQ mass spectrometer through an atmospheric pressure chemical ionization source (Thermo Scientific Waltham, MA) working in a positive mode.  $\beta$ -10'-apocarotenol was identified based on its molecular mass ( $m/z = 361.42$  [MH]<sup>+</sup>) and a fragmentation pattern of the parent ion identical with that of the  $\beta$ -10'-apocarotenol standard.

### RNA isolation

WAT was homogenized in liquid nitrogen using a liquid nitrogen cooled mortar and pestle. Total RNA was isolated using TRIzol reagent (Invitrogen, Carlsbad, CA, USA) followed by purification using RNeasy columns (Qiagen, Venlo, The Netherlands) according to the instructions of the manufacturer. RNA concentration and purity were measured using the Nanodrop spectrophotometer (ND-1000, Isogen Life Science, Maarsse, The Netherlands). Approximately 20  $\mu$ g of total RNA was isolated from each WAT depot. A260/A280 ratios were above 2 and A260/A230 ratios were above 1.9 for all samples, indicating good RNA purity. RNA degradation was checked using StdSense Chips (Biorad) and no apparent RNA degradation was seen.

### Q-PCR analysis

cDNA was prepared by reverse transcription of 1  $\mu$ g total RNA using random hexamers as primers with M-MLV reverse transcriptase (Invitrogen). The expression of selected cDNAs was analyzed by real-time quantitative PCR, as reported previously [51]. Reactions were performed in duplicate with a Stratagene MX3005P apparatus (Stratagene, Amsterdam, The Netherlands) using SYBR green kit (Eurogentec, Angers, France), according to the manufacturer instructions. Primers used were as follows: for PPAR $\gamma$ , 5'-CAA GAA TAC CAA AGT GCG ATC AA-3' and

5'-GAG CTG GGT CTT TTC AGA ATA ATA AG-3'; for RXR $\alpha$ , 5'-GCC ATC TTT GAC AGG GTG CTA-3' and 5'-CTC CGT CTT GTC CAT CTG CAT-3'; for lipoprotein lipase (LPL), 5'-GGC CAG ATT CAT CAA CTG GAT-3' and 5'-GCT CCA AGG CTG TAC CCT AAG-3'; for  $\beta$ -carotene 9', 10'-dioxygenase (Bcd2), 5'-CCT GGT GAG TAT TCC CTC ACA-3' and 5'-TCT CAA CTG TTTCTG CGT TTC-3'; and for Bcm1, 5'-TCT GAG TTC GGA ACC ATG GC-3' and 5'-GTG TGA GAC AAG TAG GAG AAA GCT-3'. The relative levels of mRNA were calculated using the comparative  $\Delta\Delta C_t$  method. 18S rRNA (5'-CGC CGC TAG AGG TGA AAT TCT-3' and 5'-CAT TCT TGG CAA ATG CTT TCG-3') was used as reference gene. For CYP26a1 mRNA quantification, the TaqMan Gene Expression Assay Mm00514486-s1 was used together with the assay Mm00507222-s1 for 18S rRNA (Applied Biosystems, Courtaboeuf, France).

### Western blot analysis

For PPAR $\gamma$  determination in iWAT, 100  $\mu$ g of total protein from each animal tissue was fractionated in SDS-polyacrylamide (12% acrylamide) and then electroblotted to a PVDF membrane. Membranes were blocked in fat-free milk (5%) dissolved in Tris buffered saline-Tween, washed and incubated overnight at 4°C with anti-mouse PPAR $\gamma$  (Abcam, Cambridge, MA) diluted 1:500. As a protein loading control,  $\beta$ -actin (Cell Signalling, Boston, MA) diluted 1:1000 was used. Secondary antibody (1:5000) was horseradish peroxidase-conjugated anti-rabbit IgG (Promega, Madison, WI). Immunoblots were developed with the ECL system (Amersham Biosciences) and scanned. Quantification of bands was performed by the ImageJ (Java).

### Microarray hybridization procedure

The 4 x 44 k Agilent whole mouse genome microarrays (G4122F, Agilent Technologies, Inc. Santa Clara, CA, USA) were used and microarray hybridization was performed essentially according to the manufacturer's protocol. In brief, cDNA was synthesized out of 1  $\mu$ g iWAT RNA using the Agilent Low RNA Input Fluorescent Linear Amplification Kit for each animal without addition of spikes. Thereafter samples were split in 2 equal amounts, to synthesize Cyanine 3-CTP (Cy3) and Cyanine 5-CTP (Cy5) labeled cRNA using half the amounts as indicated by the manufacturer per dye (Agilent Technologies) and as has been assessed previously [50]. Labeled cRNA was purified using RNeasy columns (Qiagen). Yield, A260/A280 ratio and Cy3 or Cy5 activity were examined for every sample on the nanodrop. All samples met the criteria of a cRNA yield higher than 825 ng and a specific activity of at least 8.0 pmol Cy3 or Cy5. 1200 ng of every Cy3 labeled cRNA sample was pooled and used as a common reference pool. Individual 825 ng Cy5-labeled cRNA and 825 ng pooled Cy3-labeled cRNA were fragmented in 1x fragmentation and 1x blocking agent (Agilent Technologies) at 60°C for 30 minutes and thereafter mixed with GEx Hybridization Buffer HI-RPM (Agilent Technologies) and hybridized in a 1:1 ratio at 65°C for 17 h in an Agilent Microarray hybridization chamber rotating at 4 rpm. After hybridization slides were washed according to the wash protocol with Stabilization and Drying solution (Agilent Technologies). Arrays were scanned at an Agilent scanner with 10% and 100% laser power intensities (Agilent Technologies).

### Data analyses and statistical methods

Signal intensities for each microarray spot were quantified using Feature Extraction 9.1 (Agilent Technologies). Median density values and background values of each spot were

extracted for both the experimental samples (Cy5) and the reference samples (Cy3). Quality control was performed visually, by using Quality control graphs from Feature extraction and M-A plots and boxplots were made using limmaGUI in R (Bioconductor) [52] for every microarray. Data were imported into GeneMaths XT (Applied Maths, Sint-Martens-Latem, Belgium). Spots with a Cy5 and Cy3 signal twice above background were selected and log transformed. 31295 spots had at least a 2-fold signal to noise ratio. The Cy5 signal was normalized against the Cy3 intensity as described before [53]. P-values for differential expressions were calculated between 2 groups using t-test statistics on log intensity values. Changes were considered statistically different at  $p < 0.05$ . Volcano plots were made using Graphpad Prism 5.0.2 (La Jolla, CA) with all spots or a selection of spots. Heatmapping and hierarchical clustering was performed in GeneMathsXT (Applied Maths, St. Martens Lathem, Belgium). Pathway analysis was performed using MetaCore (GeneGo Inc, St. Joseph, MI, USA). Promoter analysis and the literature based network were performed with the Genomatix suite (Genomatix Software GmbH, Germany). Biochemical and biometric parameters in Figures 1, 2, and 4 are presented as means  $\pm$  SEM. Statistical significance of effects on these parameters was assessed by two-way ANOVA and two-tailed Student's *t* test using SPSS 14.0 for windows (SPSS, Chicago, IL, USA), with threshold of significance set at  $p < 0.05$ . Microarray data has been submitted in a MIAME compliant form to Gene Expression Omnibus (GEO) data base of the National Center of Biotechnology Information (NCBI), and is accessible through GEO series accession number GSE27271 (<http://www.ncbi.nlm.nih.gov/geo/query/acc.cgi?acc=GSE27271>).

### Supporting Information

**Figure S1** (A) PPAR $\gamma$  mRNA levels, (B) RXR $\alpha$  mRNA levels, (C) lipoprotein lipase (LPL) mRNA levels, (D) Bcm1 mRNA levels and (E) Bcd2 mRNA levels in gonadal white adipose tissue of wild-type (WT) and Bcm1-null (Bcm1 $^{-/-}$ ) mice after 14 weeks on a control diet (open bars) or a  $\beta$ -carotene -enriched diet (black bars). Quantitative real-time PCR was used to determine normalized gene expression levels as described in Materials and Methods. Data are the mean  $\pm$  SEM of 6 animals per group. G, effect of genotype in two-way ANOVA analysis ( $p < 0.05$ ). (TIF)

**Table S1 Genes differentially regulated ( $p < 0.01$ ) in white adipose tissue of Bcm1 $^{-/-}$  mice after  $\beta$ -carotene supplementation.** (DOC)

**Table S2 Main pathways affected by dietary  $\beta$ -carotene supplementation in inguinal white adipose tissue of wild-type mice as indicated by Metacore analysis.** Differentially expressed genes at  $p < 0.05$  involved in aspects of metabolism as indicated are shown. (DOC)

**Table S3 Changes ( $p < 0.05$ ) in the expression of angiogenesis-related genes in inguinal white adipose tissue of wild-type and Bcm1-null mice after 14 weeks of dietary  $\beta$ -carotene supplementation.** (DOC)

**Table S4 Beta-carotene Reduces Body Adiposity of Mice via BCMO1.** (DOC)

## Acknowledgments

We thank Dr. Hansgeorg Ernst (BASF, Germany) for the gift of the  $\beta$ -10'-apo-carotenal standard and Dr. Marcin Golczak (Case Western Reserve University, Cleveland) for the help with tandem mass spectrometry analyses.

## References

- von Lintig J (2010) Colors with functions: elucidating the biochemical and molecular basis of carotenoid metabolism. *Annu Rev Nutr* 30: 35–56.
- Paik J, During A, Harrison EH, Mendelsohn CL, Lai K, et al. (2001) Expression and characterization of a murine enzyme able to cleave beta-carotene. The formation of retinoids. *J Biol Chem* 276(34): 32160–32168.
- Redmond TM, Gentleman S, Duncan T, Yu S, Wiggert B, et al. (2001) Identification, expression, and substrate specificity of a mammalian beta-carotene 15,15'-dioxygenase. *J Biol Chem* 276(9): 6560–6565.
- Kiefer C, Hessel S, Lampert JM, Vogt K, Lederer MO, et al. (2001) Identification and characterization of a mammalian enzyme catalyzing the asymmetric oxidative cleavage of provitamin A. *J Biol Chem* 276(17): 14110–14116.
- von Lintig J, Hessel S, Isken A, Kiefer C, Lampert JM, et al. (2005) Towards a better understanding of carotenoid metabolism in animals. *Biochim Biophys Acta* 1740(2): 122–131.
- von Lintig J, Vogt K (2000) Filling the gap in vitamin A research. Molecular identification of an enzyme cleaving beta-carotene to retinal. *J Biol Chem* 275(16): 11915–11920.
- Hessel S, Eichinger A, Isken A, Amengual J, Hunzelmann S, et al. (2007) CMO1 deficiency abolishes vitamin A production from beta-carotene and alters lipid metabolism in mice. *J Biol Chem* 282(46): 33553–33561.
- Fierce Y, de Moraes Vieira M, Piantedosi R, Wyss A, Blaner WS, et al. (2008) In vitro and in vivo characterization of retinoid synthesis from beta-carotene. *Arch Biochem Biophys* 472(2): 126–138.
- Lindshield BL, King JL, Wyss A, Goralczyk R, Lu CH, et al. (2008) Lycopene biodistribution is altered in 15,15'-carotenoid monooxygenase knockout mice. *J Nutr* 138(12): 2367–2371.
- Feige JN, Gelman L, Michalik L, Desvergne B, Wahli W (2006) From molecular action to physiological outputs: peroxisome proliferator-activated receptors are nuclear receptors at the crossroads of key cellular functions. *Prog Lipid Res* 45(2): 120–159.
- Grimaldi PA (2007) Peroxisome proliferator-activated receptors as sensors of fatty acids and derivatives. *Cell Mol Life Sci* 64(19–20): 2459–2464.
- Lefterova MI, Lazar MA (2009) New developments in adipogenesis. *Trends Endocrinol Metab* 20(3): 107–114.
- Boulanger A, McLemore P, Copeland NG, Gilbert DJ, Jenkins NA, et al. (2003) Identification of beta-carotene 15, 15'-monooxygenase as a peroxisome proliferator-activated receptor target gene. *Faseb J* 17(10): 1304–1306.
- Gong X, Tsai SW, Yan B, Rubin LP (2006) Cooperation between MEF2 and PPARgamma in human intestinal beta,beta-carotene 15,15'-monooxygenase gene expression. *BMC Mol Biol* 7: 7.
- Lobo GP, Amengual J, Li HN, Golczak M, Bonet ML, et al. (2010) {beta},{beta}-Carotene Decreases Peroxisome Proliferator Receptor {gamma} Activity and Reduces Lipid Storage Capacity of Adipocytes in a {beta},{beta}-Carotene Oxygenase 1-dependent Manner. *J Biol Chem* 285(36): 27891–27899.
- Ziouzenkova O, Orasanu G, Sharlach M, Akiyama TE, Berger JP, et al. (2007) Retinaldehyde represses adipogenesis and diet-induced obesity. *Nat Med* 13(6): 695–702.
- Kuri-Harcuch W (1982) Differentiation of 3T3 F442A cells into adipocytes is inhibited by retinoic acid. *Differentiation* 23: 164–169.
- Schwarz EJ, Reginato MJ, Shao D, Krakow SL, Lazar MA (1997) Retinoic acid blocks adipogenesis by inhibiting C/EBPbeta-mediated transcription. *Mol Cell Biol* 17(3): 1552–1561.
- Ribot J, Felipe F, Bonet ML, Palou A (2001) Changes of adiposity in response to vitamin A status correlate with changes of PPAR gamma 2 expression. *Obes Res* 9(8): 500–509.
- Alvarez R, de Andres J, Yubero P, Vinas O, Mampel T, et al. (1995) A novel regulatory pathway of brown fat thermogenesis. Retinoic acid is a transcriptional activator of the mitochondrial uncoupling protein gene. *J Biol Chem* 270(10): 5666–5673.
- Puigserver P, Vázquez F, Bonet ML, Picó C, Palou A (1996) In vitro and in vivo induction of brown adipocyte uncoupling protein (thermogenin) by retinoic acid. *Biochem J* 317: 827–833.
- Mercader J, Ribot J, Murano I, Felipe F, Cinti S, et al. (2006) Remodeling of white adipose tissue after retinoic Acid administration in mice. *Endocrinology* 147(11): 5325–5332.
- Mercader J, Madsen L, Felipe F, Palou A, Kristiansen K, et al. (2007) All-trans retinoic acid increases oxidative metabolism in mature adipocytes. *Cell Physiol Biochem* 20(6): 1061–1072.
- Hollung K, Rise CP, Drevon CA, Reseland JE (2004) Tissue-specific regulation of leptin expression and secretion by all-trans retinoic acid. *J Cell Biochem* 92(2): 307–315.

## Author Contributions

Conceived and designed the experiments: GL AD-K AP JK JFL MLB JvL. Performed the experiments: JA EG YJGvH SH JR EK BK-W UR. Analyzed the data: JA EG YJGvH SH JR BK-W UR. Contributed reagents/materials/analysis tools: AW JK JFL MLB JvL. Wrote the paper: MLB JvL.

- Felipe F, Bonet ML, Ribot J, Palou A (2004) Modulation of resistin expression by retinoic acid and vitamin A status. *Diabetes* 53(4): 882–889.
- Felipe F, Mercader J, Ribot J, Palou A, Bonet ML (2005) Effects of retinoic acid administration and dietary vitamin A supplementation on leptin expression in mice: lack of correlation with changes of adipose tissue mass and food intake. *Biochim Biophys Acta* 1740(2): 258–265.
- Mercader J, Granados N, Bonet ML, Palou A (2008) All-trans retinoic acid decreases murine adipose retinol binding protein 4 production. *Cell Physiol Biochem* 22(1–4): 363–372.
- Petkovich M, Brand NJ, Krust A, Chambon P (1987) A human retinoic acid receptor which belongs to the family of nuclear receptors. *Nature* 330(6147): 444–450.
- Aranda A, Pascual A (2001) Nuclear hormone receptors and gene expression. *Physiol Rev* 81(3): 1269–1304.
- Shaw N, Elholm M, Noy N (2003) Retinoic acid is a high affinity selective ligand for the peroxisome proliferator-activated receptor beta/delta. *J Biol Chem* 278(43): 41589–41592.
- Berry DC, Noy N (2009) All-trans-retinoic acid represses obesity and insulin resistance by activating both peroxisome proliferation-activated receptor beta/delta and retinoic acid receptor. *Mol Cell Biol* 29(12): 3286–3296.
- Ziouzenkova O, Orasanu G, Sukhova G, Lau E, Berger JP, et al. (2007) Asymmetric cleavage of beta-carotene yields a transcriptional repressor of retinoid X receptor and peroxisome proliferator-activated receptor responses. *Mol Endocrinol* 21(1): 77–88.
- Eroglu A, Hruszkewycz DP, Curley RW, Jr., Harrison EH ( ) The eccentric cleavage product of beta-carotene, beta-apo-13-carotenone, functions as an antagonist of RXRalpha. *Arch Biochem Biophys*. In press.
- Lijnen HR (2008) Angiogenesis and obesity. *Cardiovasc Res* 78(2): 286–293.
- Gealekman O, Burkart A, Chouinard M, Nicoloso SM, Straubhaar J, et al. (2008) Enhanced angiogenesis in obesity and in response to PPARgamma activators through adipocyte VEGF and ANGPTL4 production. *Am J Physiol Endocrinol Metab* 295(5): E1056–1064.
- Abu-Abed S, Dolle P, Metzger D, Beckett B, Chambon P, et al. (2001) The retinoic acid-metabolizing enzyme, CYP26A1, is essential for normal hindbrain patterning, vertebral identity, and development of posterior structures. *Genes Dev* 15(2): 226–240.
- Emoto Y, Wada H, Okamoto H, Kudo A, Imai Y (2005) Retinoic acid-metabolizing enzyme Cyp26a1 is essential for determining territories of hindbrain and spinal cord in zebrafish. *Dev Biol* 278(2): 415–427.
- van Helden YG, Heil SG, van Schooten EJ, Kramer E, Hessel S, et al. (2010) Knockout of the Bcmo1 gene results in an inflammatory response in female lung, which is suppressed by dietary beta-carotene. *Cell Mol Life Sci* 67(12): 2039–2056.
- Kamei Y, Kawada T, Mizukami J, Sugimoto E (1994) The prevention of adipose differentiation of 3T3-L1 cells caused by retinoic acid is elicited through retinoic acid receptor alpha. *Life Sci* 55(16): PL307–312.
- Garcia OP, Long KZ, Rosado JL (2009) Impact of micronutrient deficiencies on obesity. *Nutr Rev* 67(10): 559–572.
- Ylonen K, Alftan G, Groop L, Saloranta C, Aro A, et al. (2003) Dietary intakes and plasma concentrations of carotenoids and tocopherols in relation to glucose metabolism in subjects at high risk of type 2 diabetes: the Botnia Dietary Study. *Am J Clin Nutr* 77(6): 1434–1441.
- Coyne T, Ibiebele TI, Baade PD, Dobson A, McClintock C, et al. (2005) Diabetes mellitus and serum carotenoids: findings of a population-based study in Queensland, Australia. *Am J Clin Nutr* 82(3): 685–693.
- Ford ES, Will JC, Bowman BA, Narayan KM (1999) Diabetes mellitus and serum carotenoids: findings from the Third National Health and Nutrition Examination Survey. *Am J Epidemiol* 149(2): 168–176.
- Ramakrishna V, Jaikhanji R (2008) Oxidative stress in non-insulin-dependent diabetes mellitus (NIDDM) patients. *Acta Diabetol* 45(1): 41–46.
- Burrows TL, Warren JM, Colyvas K, Garg ML, Collins CE (2009) Validation of overweight children's fruit and vegetable intake using plasma carotenoids. *Obesity (Silver Spring)* 17(1): 162–168.
- Ferrucci L, Perry JR, Matteini A, Perola M, Tanaka T, et al. (2009) Common variation in the beta-carotene 15,15'-monooxygenase 1 gene affects circulating levels of carotenoids: a genome-wide association study. *Am J Hum Genet* 84(2): 123–133.
- Leung WC, Hessel S, Meplan C, Flint J, Oberhauser V, et al. (2009) Two common single nucleotide polymorphisms in the gene encoding {beta}-carotene 15,15'-monooxygenase alter {beta}-carotene metabolism in female volunteers. *Faseb J* 23(4): 1041–1053.

48. Lobo GP, Hessel S, Eichinger A, Noy N, Moise AR et al (2010) ISX is a retinoic acid-sensitive gatekeeper that controls intestinal beta,beta-carotene absorption and vitamin A production. *FASEB J* 24(6): 1656–1666.
49. Cinti S (2005) The adipose organ. *Prostaglandins Leukot Essent Fatty Acids* 73(1): 9–15.
50. van Schothorst EM, Pagmantidis V, de Boer VC, Hesketh J, Keijer J (2007) Assessment of reducing RNA input for Agilent oligo microarrays. *Anal Biochem* 363(2): 315–317.
51. Landrier JF, Malezet-Desmoulins C, Reboul E, Marie Lorec A, Josephe Amiot M, et al. (2008) Comparison of different vehicles to study the effect of tocopherols on gene expression in intestinal cells. *Free Radic Res* 42(5): 523–530.
52. Wettenhall JM, Smyth GK (2004) limmaGUI: a graphical user interface for linear modeling of microarray data. *Bioinformatics* 20(18): 3705–3706.
53. Pellis L, Franssen-van Hal NL, Burema J, Keijer J (2003) The intraclass correlation coefficient applied for evaluation of data correction, labeling methods, and rectal biopsy sampling in DNA microarray experiments. *Physiol Genomics* 16(1): 99–106.